NeuroImage 162 (2017) 86–92

Contents lists available at ScienceDirect

NeuroImage

journal homepage: www.elsevier.com/locate/neuroimage

Functional magnetic resonance imaging of auditory cortical fields in awake marmosets

Camille R. Toarmino [a], Cecil C.C. Yen [b], Daniel Papoti [b], Nicholas A. Bock [c], David A. Leopold [d], Cory T. Miller [a,1], Afonso C. Silva [b,*,1]

[a] Cortical Systems and Behavior Laboratory, Department of Psychology and Neurosciences Graduate Program, The University of California at San Diego, La Jolla, CA, 92093-0109, USA

[b] Cerebral Microcirculation Section, Laboratory of Functional and Molecular Imaging, National Institute of Neurological Disorders and Stroke, Bethesda, MD, 20892-4478, USA

[c] Department of Psychology, Neuroscience and Behaviour, McMaster University, Hamilton, Ontario, L8S 4K1, Canada

[d] Section on Cognitive Neurophysiology and Imaging, Laboratory of Neuropsychology, National Institute of Mental Health, Bethesda, MD, 20892-4400, USA

A B S T R A C T

The primate auditory cortex is organized into a network of anatomically and functionally distinct processing fields. Because of its tonotopic properties, the auditory core has been the main target of neurophysiological studies ranging from sensory encoding to perceptual decision-making. By comparison, the auditory belt has been less extensively studied, in part due to the fact that neurons in the belt areas prefer more complex stimuli and integrate over a wider frequency range than neurons in the core, which prefer pure tones of a single frequency. Complementary approaches, such as functional magnetic resonance imaging (fMRI), allow the anatomical identification of both the auditory core and belt and facilitate their functional characterization by rapidly testing a range of stimuli across multiple brain areas simultaneously that can be used to guide subsequent neural recordings. Bridging these technologies in primates will serve to further expand our understanding of primate audition. Here, we developed a novel preparation to test whether different areas of the auditory cortex could be identified using fMRI in common marmosets (*Callithrix jacchus*), a powerful model of the primate auditory system. We used two types of stimulation, band pass noise and pure tones, to parse apart the auditory core from surrounding secondary belt fields. In contrast to most auditory fMRI experiments in primates, we employed a continuous sampling paradigm to rapidly collect data with little deleterious effects. Here we found robust bilateral auditory cortex activation in two marmosets and unilateral activation in a third utilizing this preparation. Furthermore, we confirmed results previously reported in electrophysiology experiments, such as the tonotopic organization of the auditory core and regions activating preferentially to complex over simple stimuli. Overall, these data establish a key preparation for future research to investigate various functional properties of marmoset auditory cortex.

1. Introduction

The primate auditory cortex comprises anatomically and functionally distinct areas that form the foundation of audition (Morel et al., 1993; Rauschecker et al., 1995; Hackett et al., 1998a, 1998b; Romanski et al., 1999a; 1999b; Tian et al., 2001; for reviews see, Kaas and Hackett, 2000; Rauschecker and Tian, 2000). While neurophysiological studies show evidence for three adjacent tonotopically organized fields, A1, R, and RT (Morel et al., 1993; Aitkin et al., 1986) known as the auditory core, determining the functional contributions of secondary (belt) and tertiary (parabelt) processing fields have proven more challenging (Rauschecker et al., 1995; Rauschecker and Tian, 2004; Bendor and Wang, 2005; Tian and Rauschecker, 2004). Functional magnetic resonance imaging (fMRI) offers a complementary technique that can be used to facilitate neurophysiological research by rapidly characterizing multiple areas of the brain simultaneously and identifying patterns of responses that might not be readily identifiable with single-unit recordings (*e.g.*, Tsao et al., 2006), including the auditory system (*e.g.*, Perrodin et al., 2011). While this approach has been successfully employed in the rhesus monkey (Joly et al., 2012; Ortiz-Rios et al., 2015, 2017; Perrodin et al., 2011), its application to marmosets, a rapidly emerging model system in neuroscience (Miller et al., 2015, 2016; Miller, 2017; Bendor and Wang, 2008; Eliades and Miller, 2017), is likely to yield similarly important insights (*e.g.*, Hung et al., 2015a; 2015b). Because of the small size of the marmoset brain and acoustic interference prevalent in fMRI environments, however, it remains unclear whether distinct fields of the species

* Corresponding author. Cerebral Microcirculation Section, Laboratory of Functional and Molecular Imaging, National Institute of Neurological Disorders and Stroke, 49 Convent Drive, MSC 4478 Building 49, Room 3A72, Bethesda, MD, 20892-4478, USA.

E-mail address: SilvaA@ninds.nih.gov (A.C. Silva).

[1] Equal Contribution Senior Investigators.

http://dx.doi.org/10.1016/j.neuroimage.2017.08.052
Received 17 April 2017; Accepted 18 August 2017
Available online 19 August 2017
1053-8119/Published by Elsevier Inc.

auditory cortex could be distinguished with this method. Here we developed a novel preparation to test the suitability of fMRI for identifying small functional divisions across the marmoset auditory cortical fields.

The marmoset auditory core has been extensively explored using neurophysiological techniques (*e.g.*, Bendor and Wang, 2005; Bendor and Wang, 2008; Sadagopan and Wang, 2009; Zhou and Wang, 2012). Similarly to other primates, the species' auditory core comprises a series of three tonotopically organized fields whose borders can be identified by characteristic frequency reversals (Bendor and Wang, 2008). While these neurophysiological approaches have identified some functionally distinct areas of the marmoset auditory cortex, such as for pitch processing (Bendor and Wang, 2005; Bendor et al., 2012), delineation of the surrounding belt from the auditory core has been limited with these methods. The only previous auditory fMRI experiment in marmosets reported evidence of a vocalization selective response area (Sadagopan et al., 2015), however this study was performed in anesthetized animals, which could significantly affect the response characteristics of different auditory regions (*e.g.*, somatosensory system: Silva et al., 2011; Liu et al., 2013). It is not clear whether a study of awake marmosets would offer the level of precision evident in rhesus monkeys for identifying the auditory cortical fields (Petkov et al., 2006; Tanji et al., 2010), or if the confluence of the acoustic distortions intrinsic to the scanner environment and small brain size would severely limit the suitability of fMRI for marmoset auditory research.

In the current study, we sought to develop a preparation for imaging auditory cortex in the awake marmoset. Our goal was to replicate key findings from neurophysiological studies as a proof of principle that our preparation is effective for future fMRI research. Specifically, we aimed to reproduce frequency reversals in the auditory core (Bendor and Wang, 2008) and demonstrate selectivity for complex stimuli in the belt (Bendor and Wang, 2005; Bendor et al., 2012). We utilized a myelin atlas to illuminate the anatomical delineation of core and belt fields. Previous studies had shown that heavy myelination exists in the auditory core relative to the belt (*e.g.*, Kaas and Hackett, 2000). By registering our functional data to a myelin scan, we were able to visualize this boundary and make a coarse determination of what areas of auditory cortex were activated with specific types of stimuli. Our results reflect principles established with neurophysiological and anatomical techniques. We found frequency selective areas alternating along a caudal-rostral gradient in auditory cortex. Additionally, our results suggest that belt areas outside of the auditory core were activated to complex stimuli with our preparation. These findings establish that fMRI can be used as a complementary technique to neurophysiology to expand our understanding of the functional properties of marmoset auditory cortex.

2. Materials and methods

Magnetic resonance imaging methods. All fMRI experiments were performed in a 7T/30 cm magnet interfaced to an AVANCE AVIII MRI spectrometer (Bruker, Billerica, MA) equipped with a self-shielded 150 mm ID gradient set capable of generating 450 mT/m within 120 μs (Resonance Research Inc., Billerica, MA). An actively decoupled birdcage coil with an inner diameter of 110 mm was used as transmit coil, and the MR signal was acquired from two surface coils placed outside the helmets directly above auditory cortex. BOLD fMRI data were acquired continuously using a gradient-echo echo-planar imaging sequence (EPI). Eight slices were acquired and were oriented parallel to the lateral sulcus, as shown in Fig. 1A. Acquisition parameters for this experiment were: FOV: 2.88 × 2.88 cm^2, matrix: 96 × 96, slice thickness: 0.5 mm, resolution: 300 × 300 μm^2, TE: 26 ms, and TR: 3.6 s (Fig. 1B). All eight slices were acquired within the acquisition time TA = 462 ms so that, within each TR, a silent period of TR-TA = 3168 ms was observed during which auditory stimuli were presented. A 3.6 s TR was chosen based on peak of the marmoset hemodynamic response which is about 4 s (Liu et al., 2013).

Animal preparation. Three adult male common marmosets, weighing between 400 g and 550 g each, were used as subjects in these experiments. The subjects were adapted to the MRI scanner over a period of 30 days with a mock scanning environment described previously by Silva et al., (2011). Individualized, custom-made helmets were built (Papoti et al., 2013) to aid with head immobilization and headphone positioning. After the acclimatization period, the marmosets were scanned in fully awake conditions during all scanning sessions (Fig. 1C). Auditory stimulation was delivered bilaterally and directly into the ear canals through the use of MRI compatible headphones (STAX SR-003, Stax Ltd., Japan). Each headphone was covered with sound attenuating putty (Insta Putty Silicone Earplugs, Insta-Mold Products, Oaks, PA) in order to reduce the loudness of the scanner noise. The sound intensity level of the scanner was measured to be approximately 100 dB, with a center frequency around 2140 Hz. The putty attenuated the scanner noise by approximately 24 dB SPL. Each subject's physiological state was monitored during each scanning session by continuously acquiring its respiration rate (Biopac MP150, Biopac Systems, Inc., Goleta, CA) as well as by visual inspection of the animal via an MR compatible camera (MRC Systems, Heidelberg, Germany) placed in front of the animal's face. Experiments were in full compliance with the Animal Care and Use Committee of the National Institute of Neurological Disorders and Stroke. Complete care was taken to ensure the wellbeing of the animals involved in these experiments. Two of three monkeys performed well during scanning and exhibited minimal movement. The third monkey moved excessively, and as a result contributed only a small amount of data for this study.

Stimulus presentation. Two types of stimuli were presented in this experiment: 1) A range of pure tones (PTs) and 2) band pass noise (BPN) (Fig. 1D). PTs were varied within three different frequency bands to constitute three different types of PT stimuli (high = 4–16 kHz; medium = 1–4 kHz; and low = 0.25–1 kHz). BPN was generated by band pass filtering random noise. The center frequency of each BPN stimulus was varied within the same frequency bands to control for spectral content. The bandwidth of each type of stimulus was two octaves. A 50 ms PT was randomly generated within each frequency band followed by 50 ms of silence, such that every 100 ms a new pure tone was played within that frequency band (Fig. 1D). BPN was also modulated in this manner (Fig. 1D). All stimuli were synthesized in MATLAB (Mathworks, Inc., Natick, MA). Stimuli were presented at sound intensity levels of 75–80 dB. All stimuli were presented according to a square off-on-off block design in which stimulation periods of 36s were alternated with silence periods of 36s while BOLD fMRI data were acquired continuously (TR = 3.6s) throughout each run (see Fig. 1B). The types of stimuli chosen were based on similarity to those used in other studies across species that successfully examined tonotopy and core/belt delineations (*e.g.*, Humphries et al., 2010; Bendor and Wang, 2008; Petkov et al., 2006; Rauschecker and Tian, 2004) and were well within the hearing range of the common marmoset (125 Hz–36 kHz: Osmanski and Wang, 2011).

Data analysis. Data were preprocessed and analyzed in AFNI (Cox and Hyde, 1997). Acquired volumes were motion corrected using AFNI's function 3dvolreg. Time points with outliers were found visually and with the function 3dToutcount and removed from the analysis. Data were detrended using the function 3dBandPass. Data were registered across sessions (14 runs for Champ, 10 runs for Eli, 4 runs for Scooby) using the function 2dimreg. Runs were concatenated and underwent a multiple linear regression using the function 3dDeconvolve. Six motion regressors were added to the analysis as regressors of no interest. Data were smoothed with the function 3dBlurToFWHM at 0.5 mm. Statistical maps were thresholded at $p < 0.05$ and then cluster thresholded at a size of 10 voxels to correct for multiple comparisons using AlphaSim at an alpha value of 0.05. Voxels outside of the brain were manually segmented and masked out using ITK-SNAP (Yushkevich et al., 2006). To determine whether high and low frequency-selective regions were present in our data, we compared the activation patterns that arose from the presentation of high (4–16 kHz) PT to that of low (0.25–1 kHz) PT stimuli. To

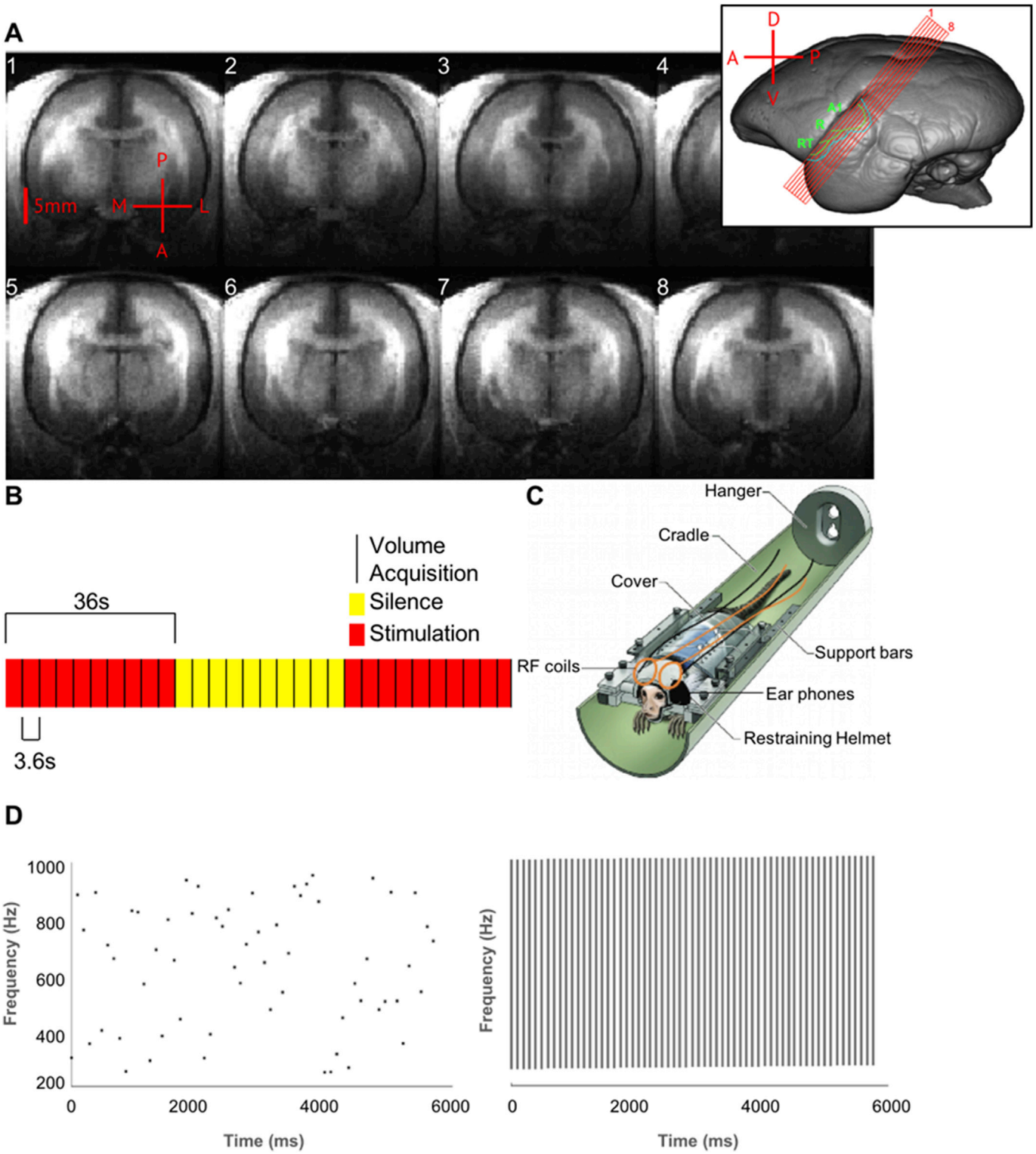

Fig. 1. **A)** Positioning of slices. Eight 0.5 mm thick slices were obtained parallel to lateral sulcus. A 3D reconstruction of one marmoset's brain is depicted with the positions of the slices overlaid. Auditory core (green) and lateral belt (blue) regions were drawn under the slices to demonstrate what was encompassed with the slice prescription. **B)** Schematic of stimulus-on-stimulus-off block design superimposed by the continuous sampling paradigm for volume acquisitions. Stimuli were presented in blocks of 36 s followed by a 36 s block of silence. MRI Volumes were acquired continuously in a clustered way every 3.6 s. **C)** Schematic of a restrained marmoset prepared for fMRI scanning adapted from Silva et al. (2011). A helmet designed to fit the contours of each individual marmoset's skull, with slots that delivered headphones directly into the ear canals, immobilized the head. Two RF coils were positioned above auditory cortex. **D)** Schematic depicting an example of the frequency content of each type of stimulus presentation. On the left, low frequency PT stimuli are presented every 50 ms with interleaving 50 ms periods of silence. On the right, low frequency BPN stimuli encompass a large spectral range on each presentation, alternating between 50 ms of stimulus and 50 ms of silence.

examine spatial selectively to BPN, we compared the activation of high BPN to high PTs.

Myelin Registration. FSL 5.0.4 was used to register a marmoset myelin atlas to an anatomical T1W scan (Bock et al., 2009) in order to visualize heavily myelinated areas that are indicative of the auditory core (Kaas and Hackett, 2000) with overlaid fMRI data. The 167 μm atlas was manually registered to the T1W anatomical and the calculated transformation was applied to the atlas. The cerebrum labels for the atlas brought it into alignment with the T1W scan.

3. Results

3.1. Activation of auditory cortex

A basic goal of this study was to use fMRI to determine the extent of auditory cortex activation in the marmoset. To this end, we began by creating functional maps contrasting blocks of broadband auditory stimulation (all stimulus types) to blocks of silence (aside from the scanner noise, see Methods). The results show robust auditory responses that activated an area roughly 7 mm by 4 mm in the three monkeys tested (Fig. 2). Two of three monkeys exhibited robust bilateral hemispheric activation, and one monkey exhibited unilateral activation ($p < 0.001$). Fig. 2D shows the time course of BOLD activity averaged across sessions for one monkey.

3.2. Parcellating the auditory core based on tonotopy

After significantly activating marmoset auditory cortex, we next sought to functionally delineate the core into its comprising ACFs. Neurophysiological studies have functionally parsed apart A1, R, and RT by examining the characteristic frequency reversals of these regions (*e.g.*, Bendor and Wang, 2008). These studies have shown that A1 and R share a low frequency border and R and RT share a high frequency border. To spatially parcellate these regions, we used three groups of random frequencies of different bandwidths as stimulation (see 'Stimulus presentation' under Methods for detail): low (0.25–1 kHz), medium (1–4 kHz), and high (4–16 kHz).

We observed distinct spatial patterns of voxels that were selective for high and low frequencies (Fig. 3, $p < 0.001$). High frequencies were located mostly caudally in A1 (Fig. 3A, slices 2–3) and at the border of R and RT (Fig. 3A, slices 2–4), while low frequencies were found at the border of A1 and R (Fig. 3A, slice 3) and in more rostral and lateral regions of RT (Fig. 3A, slices 2–4). The BOLD time courses (Fig. 3C) showed a modulation of the intensity of activation such that activated voxels within the high frequency regions responded stronger to high frequency PTs than to lower frequency PTs (Fig. 3C, blue time course). Conversely, activated voxels within the low frequency regions responded stronger to low frequency PTs than to high frequency PTs (Fig. 3C, orange time course).

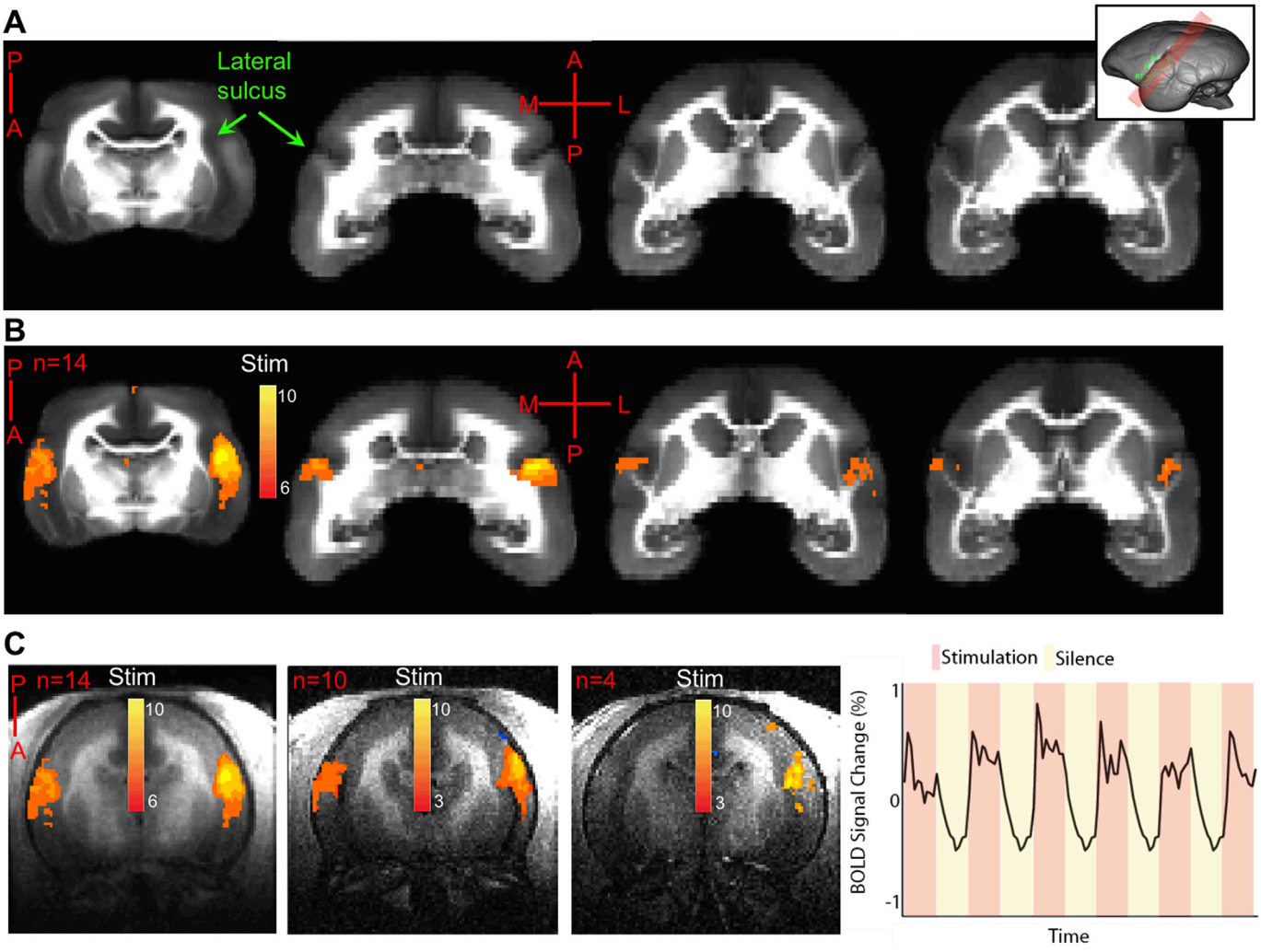

Fig. 2. Auditory cortex activation. A) Exemplar coronal and axial myelin slices demonstrating the location of lateral sulci. B) Functional activation map from one monkey showing robust bilateral auditory cortex activation to all stimuli. C) Left: Functional activation maps overlaid on T1W anatomical scans for three different monkeys. Right: Time course of BOLD signal change (%) during epochs of auditory stimulation and silence. A = anterior; P = posterior; M = medial; L = latera.

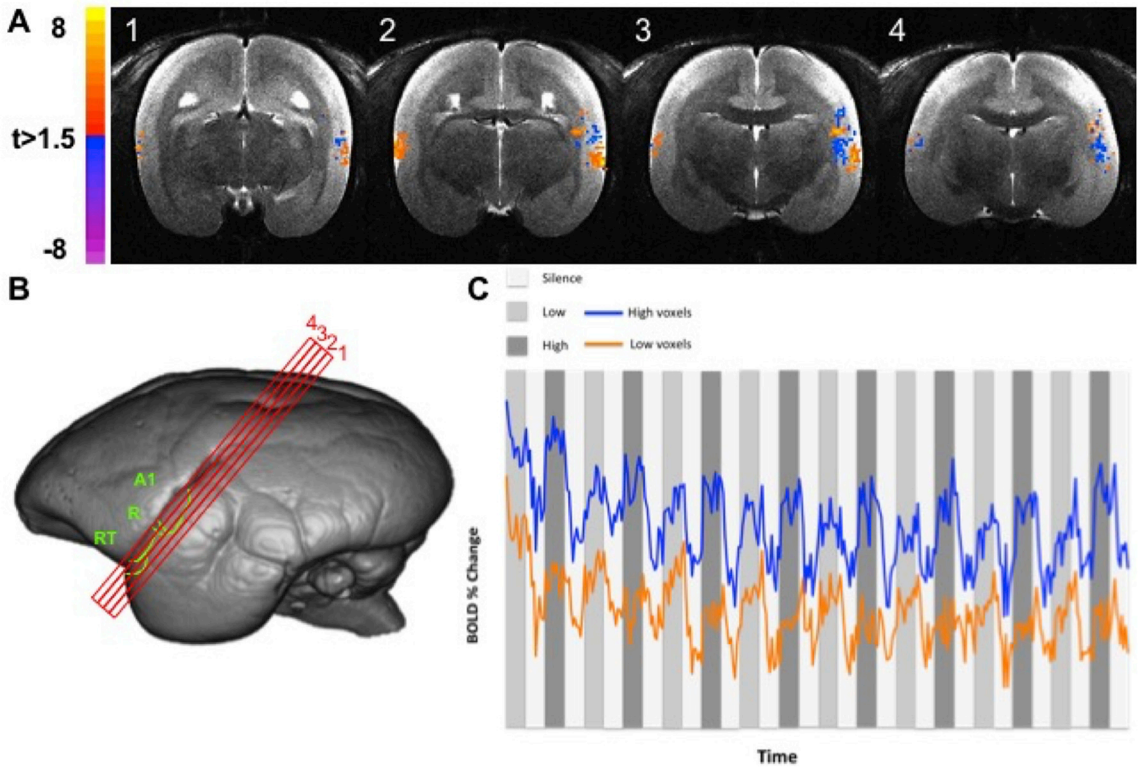

Fig. 3. (A) Frequency selective functional activation maps of the marmoset brain overlaid onto four consecutive T2-weighted MRI slices acquired parallel to the lateral sulcus as indicated in (B). The activation maps show voxels that respond selectively to pure tones at low (purple-blue, 0.25–1 kHz) and high (red-yellow, 4–16 kHz) frequencies. High frequencies were located mostly caudally in A1 (slices 2–3) and at the border of R and RT (slices 2–4), while low frequencies were found at the border of A1 and R (slice 3) and in more rostral and lateral regions of RT (slices 2–4). (C) Time course of BOLD signal changes from the activated voxels responding to high frequencies (blue time course) and to low frequencies (orange time course). Data are from one exemplar monkey, the same monkey that provided data for Fig. 2B.

3.3. Parcellating core and belt auditory regions based on stimulus type

Next we sought to functionally distinguish the auditory core (A1, R, RT) from belt regions. We compared the activation of high BPN to high PTs (see 'Stimulus presentation' under Methods) and found areas that were significantly more activated by BPN ($p < 0.01$, Fig. 4) located posterior and laterally. The myelin atlas is pertinent to interpreting our results. These data were registered to a myelin scan in order to visualize areas of greater and lesser myelination. Due to its heavy myelination (Kaas and Hackett, 2000), the lighter areas indicate a coarse estimation of the location of the auditory core. As the lighter areas transition to darker areas, this likely indicates the boundary between the core and the belt.

4. Discussion

Recent development of functional neuroimaging techniques, such as fMRI, provides a complementary tool to neurophysiology studies for efficiently mapping the functional contributions of many ACFs for acoustic signal processing and auditory perception. Here we sought to develop a fMRI preparation to investigate these issues in awake marmosets using high-resolution (7T) imaging. Analyses revealed that strong activation of auditory fields in marmosets is possible using the preparation developed here. Furthermore, we were able to replicate two representative properties of auditory cortex found using single-unit neurophysiological techniques. Our results revealed tonotopic separation

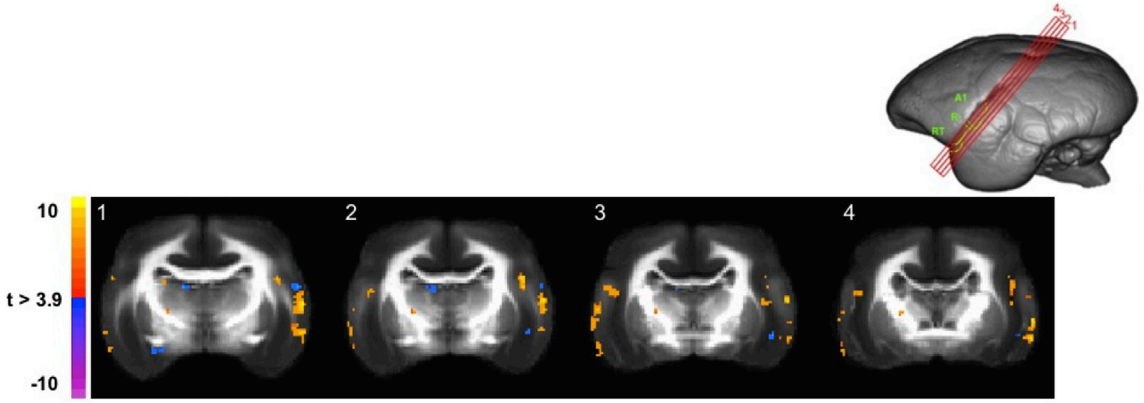

Fig. 4. BPN (orange) and PT (blue) functional activation maps of the marmoset brain overlaid onto four consecutive T1-weighted myelin MRI slices acquired parallel to the lateral sulcus as indicated in the inset. PT selective voxels were located mostly caudally in the auditory core (A1, slices 1–2) and in more rostral regions of the medial belt (slices 2–4), while BPN selective voxels were found at both lateral and medial areas of the belt surrounding A1, RT and R (slices 1–4). Data are from one exemplar monkey, the same monkey that provided data for Fig. 2B.

of auditory fields within the auditory core using pure tone stimuli and stronger response for noise stimuli in the belt region relative to core. Replicating these principles served as an indicator that our imaging and stimulation preparations were effective. Overall, this study demonstrates that fMRI in marmosets can be a powerful tool to explicate the functional anatomy of primate auditory cortex.

Tonotopic representation of frequencies is a fundamental principle of the auditory system beginning in the cochlea with frequency selectivity maintained to the level of the cortex (Russell and Sellick, 1977; Miller et al., 2001). In the past, neurophysiological studies in primates have functionally delineated the core by taking advantage of the tonotopy within the core and the mirror frequency reversals at the borders of the different fields (Merzenich and Brugge, 1973; Morel et al., 1993; Bendor and Wang, 2008). These studies have demonstrated that frequency selectivity is located on a caudal to rostral axis with high frequencies located most caudally in A1, a low frequency border at A1 and R, a high frequency border at R and RT, and low frequencies located most rostral and laterally. Our analyses showed that high frequency voxels were located caudally in A1 and at the border of R and RT, while low frequency voxels were located at the border of A1 and R and in the rostral end of RT. Therefore, our results presented in Fig. 3 confirm the general tonotopic organization of the primate auditory cortex described in the previous studies (Merzenich and Brugge, 1973; Morel et al., 1993; Kaas and Hackett, 2000), including in marmosets (Bendor and Wang, 2008). However, we did not find any voxels that were selective to medium frequencies (1–4 kHz), likely due to the effect of the continuous scanner noise (~2 kHz) on the auditory signal.

Auditory cortical belt regions are thought to be secondary stages of auditory processing once the signal reaches the cortical level. The lateral belt has direct reciprocal connections to the core and exhibits organized frequency selectivity (Hackett et al., 1998a; 1998b; Kaas and Hackett, 2000). Neurophysiological experiments found that while neurons in the core are responsive primarily to narrow band tones, lateral belt neurons are tuned to stimuli with a broader frequency spectrum, such as band-passed noise or species-specific vocalizations (Rauschecker et al., 1995; Recanzone et al., 2000; Joly et al., 2012). In the present study, we functionally distinguished the auditory core from the belt in a similar manner. Presenting band-passed noise and pure tone frequencies of matched bandwidths as stimuli indicated that the lateral belt exhibited greater activation to the noise stimuli. This confirms findings from neurophysiological studies that demonstrate that the lateral belt is more strongly tuned to stimuli with broader bandwidths than pure tones.

Results presented here are consistent with investigations of auditory function in other nonhuman primates and humans. Studies utilizing fMRI in rhesus macaques report similar findings to the present study. In the most extensive study, Petkov et al. (2006) presented tones and band-passed noise stimuli to awake and anesthetized rhesus monkeys in a similar manner and found a distinction between core and belt areas. Likewise, they reported tonotopic organization characteristic of core as well as frequency reversals that differentiate A1, R and RT. In a study that tested the effects of sound levels on tonotopic representations in rhesus monkeys, Tanji et al. (2010) confirmed the caudo-rostral orientation of frequency reported by Petkov et al. (2006) and demonstrated that increasing sound levels decreases frequency selectivity, although frequency reversals were still present. Human studies reported similar belt and core distinctions (Formisano et al., 2003; Wessinger et al., 2001) as well as frequency selectivity organized in a tonotopic fashion (*e.g.*, Humphries et al., 2010; Leaver and Rauschecker, 2016). Overall, these studies suggest conservation in the organization of auditory cortex across human and nonhuman primates. The ability to compare neural functioning across species is one key advantage to utilizing fMRI in studies of auditory processing. Future studies might examine functional properties of marmoset auditory cortex observed in other species, such as frequency selectivity in belt regions as seen in macaques (Rauschecker et al., 1995), or encoding to natural sounds (humans: Moerel et al., 2013; Santoro et al., 2014).

A serious challenge posed for fMRI experiments testing auditory function is, as the MR signal is acquired, the scanner emits bursts of loud acoustic noise as the gradient coil is switched. This constant sound could potentially interact with and compromise the auditory signal of interest. To address this issue, many scientists have employed the use of sparse temporal sampling paradigms that acquire volumes at the end of stimulation near the max of the hemodynamic response and have long intervals between samples (Bandettini et al., 1998; Gaab et al., 2007; Schmidt et al., 2008). Although these paradigms are designed to avoid scanner noise interference with the auditory signal of interest, they typically require more samples as a result of long TR. An alternative is the use of continuous sampling in which images are acquired at very short intervals throughout the entire length of the experiment. A major advantage of this paradigm is that is maximizes the number of volumes that can be acquired within an experiment, although the effect of the noise is less clear. Tanji et al. (2010) demonstrated that tonotopic maps could be successfully acquired in macaques using a continuous sampling paradigm. These maps were similar to those reported by Petkov et al. (2006), who utilized a sparse sampling paradigm. The current study utilized continuous sampling with clustered data acquisition for a short acquisition time TA within the long repetition time TR revealed a robust change in the BOLD signal during epochs of stimulation compared with epochs of silence in three monkeys (Figs. 2–3). This change was statistically significant, suggesting that the continuous sampling paradigm developed is an effective paradigm to obtain broad auditory cortex activation in common marmosets, despite potentially deleterious scanner noise interference. However, unexpectedly, we did not find any voxels selective to medium frequencies, likely due to the scanner noise interfering with that specific range of frequencies. Continuous-clustered sampling may be highly effective and useful depending on the frequency composition of the specific stimuli used in an experiment.

Although marmosets have recently garnered significant interest as a neuroscientific model (Mitchell et al., 2014; Miller, 2017; Miller et al., 2016), this species has a long history as an important model in the auditory system (Bendor and Wang, 2005; Bendor and Wang, 2008; Sadagopan and Wang, 2009; Zhou and Wang, 2012). By using high-resolution (7T) fMRI to identify distinct auditory cortical fields in awake marmosets, we show that this technique can complement existing neurophysiological experiments to expand our understanding of the primate auditory system. Similarly to recent fMRI experiments in marmoset vision (Hung et al., 2015a, 2015b) and somatosensory cortex (Yen et al., 2017), this preparation is amenable to techniques involving conditioned behavior and can, therefore, be extended to investigate relative contributions of multiple auditory cortical fields during behaviorally-dependent facets of audition (Remington et al., 2012; Song et al., 2016). Given the significance of marmosets as a neurobiological model of communication (Toarmino et al., 2017; Eliades and Wang, 2013; Miller et al., 2015; Eliades and Miller, 2017; Miller, 2017; Nummela et al., 2017), our approach could be implemented to identify areas of the auditory cortical system involved in vocalization processing (*e.g.*, Sadagopan et al., 2015; Perrodin et al., 2011). Together, these approaches can shed light on auditory function in ways not previously possible.

Conflicts of interest

The authors declare no competing financial interests.

Acknowledgements

This research was funded,in part, by the Intramural Research Program of the NIH, NINDS (Alan P. Koretsky, Scientific Director), and by the Extramural Research Program of the NIH, NIDCD (Principal Investigator: Cory T. Miller, grant R01DC012087). The authors are grateful to Xianfeng Zhang, Julie Mackel and Jennifer Ciuchta for technical assistance with animal preparation, and to Cirong Liu for assistance with data processing.

References

Aitkin, L.M., Merzenich, M.M., Irvine, D.R., Clarey, J.C., Nelson, J.E., 1986. Frequency representation in auditory cortex of the common marmoset (Callithrix jacchus jacchus). J. Comp. Neurol. 252 (2), 175–185.

Bandettini, P.A., Jesmanowicz, A., Van Kylen, J., Birn, R.M., Hyde, J.S., 1998. Functional MRI of brain activation induced by scanner acoustic noise. Magn. Reson. Med. 39 (3), 410–416.

Bendor, D., Osmanski, M.S., Wang, X., 2012. Dual-pitch processing mechanisms in primate auditory cortex. J. Neurosci. 32 (46), 16149–16161.

Bendor, D., Wang, X., 2008. Neural response properties of primary, rostral, and rostrotemporal core fields in the auditory cortex of marmoset monkeys. J. Neurophysiol. 100 (2), 888–906.

Bendor, D., Wang, X., 2005. The neuronal representation of pitch in primate auditory cortex. Nature 436 (7054), 1161–1165.

Bock, N.A., Kocharyan, A., Liu, J.V., Silva, A.C., 2009. Visualizing the entire cortical myelination pattern in marmosets with magnetic resonance imaging. J. Neurosci. Meth. 185 (1), 15–22.

Cox, R.W., Hyde, J.S., 1997. Software tools for analysis and visualization of fMRI data. NMR Biomed. 10 (45), 171–178.

Eliades, S.J., Miller, C.T., 2017. Marmoset Vocal communication: behavior and neurobiology. Dev. Neurobiol. 77 (3), 286–299.

Eliades, S.J., Wang, X., 2013. Comparison of auditory-vocal interactions across multiple types of vocalizations in marmoset auditory cortex. J. Neurophysiol. 109 (6), 1638–1657.

Formisano, E., Kim, D.S., Di Salle, F., van de Moortele, P.F., Ugurbil, K., Goebel, R., 2003. Mirror-symmetric tonotopic maps in human primary auditory cortex. Neuron 40 (4), 859–869.

Gaab, N., Gabrieli, J.D., Glover, G.H., 2007. Assessing the influence of scanner background noise on auditory processing. II. An fMRI study comparing auditory processing in the absence and presence of recorded scanner noise using a sparse design. Hum. Brain Mapp. 28 (8), 721–732.

Hackett, T.A., Stepniewska, I., Kaas, J.H., 1998a. Subdivisions of auditory cortex and ipsilateral cortical connections of the parabelt auditory cortex in macaque monkeys. J. Comp. Neurol. 394 (4), 475–495.

Hackett, T.A., Stepniewska, I., Kaas, J.H., 1998b. Thalamocortical connections of the parabelt auditory cortex in macaque monkeys. J. Comp. Neurol. 400 (2), 271–286.

Humphries, C., Liebenthal, E., Binder, J.R., 2010. Tonotopic organization of human auditory cortex. Neuroimage 50 (3), 1202–1211.

Hung, C.C., Yen, C.C., Ciuchta, J.L., Papoti, D., Bock, N.A., Leopold, D.A., Silva, A.C., 2015a. Functional mapping of face-selective regions in the extrastriate visual cortex of the marmoset. J. Neurosci. 35 (3), 1160–1172.

Hung, C.C., Yen, C.C., Ciuchta, J.L., Papoti, D., Bock, N.A., Leopold, D.A., Silva, A.C., 2015b. Functional MRI of visual responses in the awake, behaving marmoset. Neuroimage 120, 1–11.

Joly, O., Ramus, F., Pressnitzer, D., Vanduffel, W., Orban, G.A., 2012. Interhemispheric differences in auditory processing revealed by fMRI in awake rhesus monkeys. Cerebr. Cortex 22 (4), 838–853.

Kaas, J.H., Hackett, T.A., 2000. Subdivisions of auditory cortex and processing streams in primates. Proc. Natl. Acad. Sci. 97 (22), 11793–11799.

Leaver, A.M., Rauschecker, J.P., 2016. Functional topography of human auditory cortex. J. Neurosci. 36 (4), 1416–1428.

Liu, J.V., Hirano, Y., Nascimento, G.C., Stefanovic, B., Leopold, D.A., Silva, A.C., 2013. fMRI in the awake marmoset: somatosensory-evoked responses, functional connectivity, and comparison with propofol anesthesia. Neuroimage 78, 186–195.

Merzenich, M.M., Brugge, J.F., 1973. Representation of the cochlear partition on the superior temporal plane of the macaque monkey. Brain Res. 50 (2), 275–296.

Miller, C.T., 2017. Why marmosets? Dev. Neurobiol. 77 (3), 237–243.

Miller, L.M., Escabõ, M.A., Read, H.L., Schreiner, C.E., 2001. Functional convergence of response properties in the auditory thalamocortical system. Neuron 32 (1), 151–160.

Miller, C.T., Freiwald, W.A., Leopold, D.A., Mitchell, J.F., Silva, A.C., Wang, X., 2016. Marmosets: a neuroscientific model of human social behavior. Neuron 90 (2), 219–233.

Miller, C.T., Thomas, A.W., Nummela, S.U., Lisa, A., 2015. Responses of primate frontal cortex neurons during natural vocal communication. J. Neurophysiol. 114 (2), 1158–1171.

Mitchell, J.F., Reynolds, J.H., Miller, C.T., 2014. Active vision in marmosets: a model system for visual neuroscience. J. Neurosci. 34 (4), 1183–1194.

Moerel, M., De Martino, F., Santoro, R., Ugurbil, K., Goebel, R., Yacoub, E., Formisano, E., 2013. Processing of natural sounds: characterization of multipeak spectral tuning in human auditory cortex. J. Neurosci. 33 (29), 11888–11898.

Morel, A., Garraghty, P.E., Kaas, J.H., 1993. Tonotopic organization, architectonic fields, and connections of auditory cortex in macaque monkeys. J. Comp. Neurol. 335 (3), 437–459.

Nummela, S.U., Jovanovic, V., de la Mothe, L., Miller, C.T., 2017. Social context-dependent activity in marmoset frontal cortex populations during natural conversations. J. Neurosci. 37 (29), 7036–7047.

Ortiz-Rios, M., Azevedo, F.A., Kuśmierek, P., Balla, D.Z., Munk, M.H., Keliris, G.A., Rauschecker, J.P., 2017. Widespread and opponent fMRI signals represent sound location in macaque auditory cortex. Neuron 93 (4), 971–983.

Ortiz-Rios, M., Kuśmierek, P., DeWitt, I., Archakov, D., Azevedo, F.A., Sams, M., Rauschecker, J.P., 2015. Functional MRI of the vocalization-processing network in the macaque brain. Front. Neurosci. 9.

Osmanski, M.S., Wang, X., 2011. Measurement of absolute auditory thresholds in the common marmoset (Callithrix jacchus). Hear. Res. 277 (1), 127–133.

Papoti, D., Yen, C.C., Mackel, J.B., Merkle, H., Silva, A.C., 2013. An embedded four-channel receive-only RF coil array for fMRI experiments of the somatosensory pathway in conscious awake marmosets. NMR Biomed. 26 (11), 1395–1402.

Perrodin, C., Kayser, C., Logothetis, N.K., Petkov, C.I., 2011. Voice cells in the primate temporal lobe. Curr. Biol. 21 (16), 1408–1415.

Petkov, C.I., Kayser, C., Augath, M., Logothetis, N.K., 2006. Functional imaging reveals numerous fields in the monkey auditory cortex. PLoS Biol. 4 (7), e215.

Rauschecker, J.P., Tian, B., 2000. Mechanisms and streams for processing of "what" and "where" in auditory cortex. Proc. Natl. Acad. Sci. 97 (22), 11800–11806.

Rauschecker, J.P., Tian, B., 2004. Processing of band-passed noise in the lateral auditory belt cortex of the rhesus monkey. J. Neurophysiol. 91 (6), 2578–2589.

Rauschecker, J.P., Tian, B., Hauser, M., 1995. Processing of complex sounds in the macaque nonprimary auditory cortex. Science 268 (5207), 111.

Recanzone, G.H., Guard, D.C., Phan, M.L., Su, T.I.K., 2000. Correlation between the activity of single auditory cortical neurons and sound-localization behavior in the macaque monkey. J. Neurophysiol. 83 (5), 2723–2739.

Remington, E.D., Osmanski, M.S., Wang, X., 2012. An operant conditioning method for studying auditory behaviors in marmoset monkeys. PLoS One 7 (10), e47895.

Romanski, L.M., Bates, J.F., Goldman-Rakic, P.S., 1999a. Auditory belt and parabelt projections to the prefrontal cortex in the rhesus monkey. J. Comp. Neurol. 403 (2), 141–157.

Romanski, L.M., Tian, B., Fritz, J., Mishkin, M., Goldman-Rakic, P.S., Rauschecker, J.P., 1999b. Dual streams of auditory afferents target multiple domains in the primate prefrontal cortex. Nat. Neurosci. 2 (12), 1131–1136.

Russell, I.J., Sellick, P.M., 1977. Tuning properties of cochlear hair cells. Nature 267 (5614), 858–860.

Sadagopan, S., Temiz-Karayol, N.Z., Voss, H.U., 2015. High-field functional magnetic resonance imaging of vocalization processing in marmosets. Sci. Rep. 5.

Sadagopan, S., Wang, X., 2009. Nonlinear spectrotemporal interactions underlying selectivity for complex sounds in auditory cortex. J. Neurosci. 29 (36), 11192–11202.

Santoro, R., Moerel, M., De Martino, F., Goebel, R., Ugurbil, K., Yacoub, E., Formisano, E., 2014. Encoding of natural sounds at multiple spectral and temporal resolutions in the human auditory cortex. PLoS Comput. Biol. 10 (1), e1003412.

Schmidt, C.F., Zaehle, T., Meyer, M., Geiser, E., Boesiger, P., Jancke, L., 2008. Silent and continuous fMRI scanning differentially modulate activation in an auditory language comprehension task. Hum. Brain Mapp. 29 (1), 46–56.

Silva, A.C., Liu, J.V., Hirano, Y., Leoni, R.F., Merkle, H., Mackel, J.B., Zhang, X.F., Nascimento, G.C., Stefanovic, B., 2011. Longitudinal functional magnetic resonance imaging in animal models. Methods Mol. Biol. **711**, 281–302.

Song, X., Osmanski, M.S., Guo, Y., Wang, X., 2016. Complex pitch perception mechanisms are shared by humans and a new world monkey. Proc. Natl. Acad. Sci. 113 (3), 781–786.

Tanji, K., Leopold, D.A., Frank, Q.Y., Zhu, C., Malloy, M., Saunders, R.C., Mishkin, M., 2010. Effect of sound intensity on tonotopic fMRI maps in the unanesthetized monkey. Neuroimage 49 (1), 150–157.

Tian, B., Rauschecker, J.P., 2004. Processing of frequency-modulated sounds in the lateral auditory belt cortex of the rhesus monkey. J. Neurophysiol. 92 (5), 2993–3013.

Tian, B., Reser, D., Durham, A., Kustov, A., Rauschecker, J.P., 2001. Functional specialization in rhesus monkey auditory cortex. Science 292 (5515), 290–293.

Tsao, D.Y., Freiwald, W.A., Tootell, R.B., Livingstone, M.S., 2006. A cortical region consisting entirely of face-selective cells. Science 311 (5761), 670–674.

Toarmino, C.R., Wong, L., Miller, C.T., 2017. Audience affects decision-making in a marmoset communication network. Biol. Lett. 13 (1), 20160934.

Wessinger, C.M., VanMeter, J., Tian, B., Van Lare, J., Pekar, J., Rauschecker, J.P., 2001. Hierarchical organization of the human auditory cortex revealed by functional magnetic resonance imaging. J. Cognit. Neurosci. 13 (1), 1–7.

Yen, C.C., Papoti, D., Silva, A.C., 2017. Investigating the spatiotemporal characteristics of the deoxyhemoglobin- related and deoxyhemoglobin-unrelated functional hemodynamic response across cortical layers in awake marmosets. Neuroimage. http://dx.doi.org/10.1016/j.neuroimage.2017.03.005.

Yushkevich, P.A., Piven, J., Hazlett, H.C., Smith, R.G., Ho, S., Gee, J.C., Gerig, G., 2006. User-guided 3D active contour segmentation of anatomical structures: significantly improved efficiency and reliability. Neuroimage 31 (3), 1116–1128.

Zhou, Y., Wang, X., 2012. Level dependence of spatial processing in the primate auditory cortex. J. Neurophysiol. 108 (3), 810–826.